



Published in final edited form as:

*Dent Mater.* 2016 April ; 32(4): 499–509. doi:10.1016/j.dental.2015.12.005.

## Fatigue Resistance of CAD/CAM Resin Composite Molar Crowns

Fatma A. Shembish<sup>1</sup>, Hui Tong<sup>1,2</sup>, Marina Kaizer<sup>1,3</sup>, Malvin N. Janal<sup>4</sup>, Van P. Thompson<sup>5</sup>, Niek J. Opdam<sup>6</sup>, and Yu Zhang<sup>1,\*</sup>

<sup>1</sup>Department of Biomaterials and Biomimetics, New York University College of Dentistry, 433 First Avenue, New York, NY 10010, USA <sup>2</sup>School of Metallurgy and Environment, Central South University, Changsha, Hunan 410083, P.R. China <sup>3</sup>Graduate Program in Dentistry, Federal University of Pelotas, Pelotas, Brazil <sup>4</sup>Department of Epidemiology and Health Promotion, New York University College of Dentistry <sup>5</sup>Biomaterials, Biomimetics and Biophotonics, King's College London Dental Institute <sup>6</sup>Radboud University Nijmegen Medical Centre, College of Dental Sciences, Preventive and Restorative Dentistry, Ph van Leydenlaan 25, PO Box 9101 6500HB Nijmegen, The Netherlands

### Abstract

**Objective**—To demonstrate the fatigue behavior of CAD/CAM resin composite molar crowns using a mouth-motion step-stress fatigue test. Monolithic leucite-reinforced glass-ceramic crowns were used as a reference.

**Methods**—Fully anatomically shaped monolithic resin composite molar crowns (Lava Ultimate,  $n = 24$ ) and leucite reinforced glass-ceramic crowns (IPS Empress CAD,  $n = 24$ ) were fabricated using CAD/CAM systems. Crowns were cemented on aged dentin-like resin composite tooth replicas (Filtek Z100) with resin-based cements (RelyX Ultimate for Lava Ultimate or Multilink Automix for IPS Empress). Three step-stress profiles (aggressive, moderate and mild) were employed for the accelerated sliding-contact mouth-motion fatigue test. Twenty one crowns from each group were randomly distributed among these three profiles (1:2:4). Failure was designated as chip-off or bulk fracture. Optical and electronic microscopes were used to examine the occlusal surface and subsurface damages, as well as the material microstructures.

**Results**—The resin composite crowns showed only minor occlusal damage during mouth-motion step-stress fatigue loading up to 1700 N. Cross-sectional views revealed contact-induced cone cracks in all specimens, and flexural radial cracks in 2 crowns. Both cone and radial cracks were relatively small compared to the crown thickness. Extending these cracks to the threshold for

\*Corresponding author. Yu Zhang, Address: Department of Biomaterials and Biomimetics, New York University College of Dentistry, 433 First Avenue, Room 810, New York, NY 10010, USA Tel.: + 1 212 998 9637; fax: + 1 212 995 4244. yz21@nyu.edu (Y. Zhang).

**Publisher's Disclaimer:** This is a PDF file of an unedited manuscript that has been accepted for publication. As a service to our customers we are providing this early version of the manuscript. The manuscript will undergo copyediting, typesetting, and review of the resulting proof before it is published in its final citable form. Please note that during the production process errors may be discovered which could affect the content, and all legal disclaimers that apply to the journal pertain.

### Conflict of Interest

All authors declare no conflict of interest.

catastrophic failure would require much higher indentation loads or more loading cycles. In contrast, all of the glass-ceramic crowns fractured, starting at loads of approximately 450 N.

**Significance**—Monolithic CAD/CAM resin composite crowns endure, with only superficial damage, fatigue loads 3 – 4 times higher than those causing catastrophic failure in glass-ceramic CAD crowns.

### Keywords

Fatigue; fracture; resin composite; glass-ceramic; CAD/CAM crowns; Weibull analysis

---

## 1 Introduction

In clinical dentistry, there is a shift towards placing metal-free restorations. For direct restorations, resin composite has become the standard material that, depending on risk factors of tooth and patient, provides restorations with good longevity [1–3]. Indirect restorations allow the dentist greater control of the form and function of a restoration, especially for teeth with considerable amount of tooth substance loss. For indirect restorations, several types of ceramic restorative materials have shown good survival rates when applied as full coverage crowns or inlays, although chipping of the ceramic remains a common problem [4, 5]. Indirect resin composite restorations have shown acceptable survivability [6, 7], but their performance is not better than direct restorations [8]. The increased use of resin composite materials for indirect restorations follows from several recent trends: significant improvements in their mechanical properties, increased demands for highly esthetic, metal-free, biocompatible restorations [9, 10], and rapid advances in computer-aided design/computer-assisted manufacturing (CAD/CAM) technology. Recently, resin composite blocks have been introduced for use with CAD/CAM systems as an alternative for machinable ceramics [11]. CAD/CAM resin composite restorations have several advantages over their ceramic counterparts: (1) Resin composite blocks are milling damage tolerant, which allows for a faster milling speed and provides better marginal quality [12]; a full contour crown takes only 6 minutes to mill [13]! (2) No post-milling firing is needed. (3) Indirect resin composite restorations can be easily polished and adjusted for proper occlusion. These properties permit the fabrication and placement of a complete restoration within a single dental office visit [13, 14], benefiting both the patient and practitioner.

Much effort has been made to improve the mechanical properties of resin composite restorative materials, such as increased filler content, changes in filler particle size and shape, changes in matrix composition, and improvements of polymerization methods [15–19]. Recently, nanotechnology has been introduced to the dental resin composite manufacturing field. One recently developed nanohybrid resin composite material is Lava Ultimate CAD/CAM Restorative (3M ESPE, St. Paul, MI, USA); it is heat-cured through a proprietary manufacturing process, which eliminates the need for any further polymerization after milling.

Several in vitro studies have evaluated indirect resin composites. Magne and colleagues conducted a number of studies on Paradigm MZ100 (3M ESPE) [20–22]. They compared

the fatigue resistance of resin composite and ceramic occlusal veneers and onlays with various thicknesses on posterior teeth (some with endodontic treatments). They reported that posterior occlusal veneers and onlays made of MZ100 had significantly higher fatigue resistance compared to IPS Empress CAD (Ivoclar Vivadent, Schaan, Liechtenstein), IPS e.max CAD (Ivoclar Vivadent), and Vitablocks Mark II (VITA Zahnfabrik, Bad Säckingen, Germany). Kassem et al. [23] examined the effect of cyclic loading using a hardened steel ball ( $r = 3$  mm) on fatigue resistance and microleakage of monolithic CAD/CAM molar ceramic and resin composite crowns. Their results revealed that MZ100 resin composite molar crowns were more fatigue resistant than Vitablocks Mark II ceramic crowns, after 1,000,000 cycles of cyclic loading at 600 N. However, ceramic crowns exhibited significantly less microleakage relative to resin composite crowns, irrespective of the type of the cement used. Belli et al. [24] compared the fatigue resistance of modern dental ceramic bar specimens versus resin composites using the 4-point bending method. Their results revealed that while resin composite and dental ceramics exhibit similar fatigue degradation, resin composite materials used for direct restorations are more resistant to cyclic flexural loading than glass-rich ceramics used for indirect restorations. Johnson et al. [25] showed superior fracture strength of posterior occlusal veneers made from Lava Ultimate resin composites than Paradigm MZ100 and concluded that Lava Ultimate were able to survive higher occlusal loads than MZ100.

By introducing the new and improved indirect nanohybrid resin composite material, the clinical indications of CAD/CAM resin composite restoration have been extended to full coverage posterior crowns, which require greater mechanical integrity than inlays and onlays. However, to our knowledge, no *in vitro* fatigue study has been conducted on full-coverage posterior nanohybrid resin composite crowns. The purpose of this *in vitro* study is, therefore, to investigate the sliding contact mouth-motion fatigue behavior and reliability of a newly developed indirect nanohybrid resin composite (Lava Ultimate) for posterior crown applications.

## 2 Materials and Methods

### 2.1 Crown Fabrication

Anatomically correct mandibular first molar crowns ( $n = 24$ , resin composite Lava Ultimate crowns;  $n = 24$ , glass-ceramic IPS Empress CAD crowns) were designed and milled from CAD/CAM blocks using the following systems: Lava Milling System (3M ESPE) in a 3M certified dental lab (Jensen Dental, North Haven, CT) and CEREC System (Sirona, Charlotte, NC, USA). A standard die of a mandibular first molar preparation was scanned into the system adjusted to compensate for the cement layer thickness (50  $\mu$ m). Tooth preparation was modeled by reducing the proximal walls by 1.5 mm and the occlusal surface by 2.0 mm. After milling the crowns were processed according to the manufacturer recommendation: (1) Lava Ultimate – polished with Meisinger Luster and diamond paste (Meisinger, Centennial, CO, USA); (2) IPS Empress CAD – glazed with IPS Empress Universal Glaze (Ivoclar Vivadent).

## 2.2 Cementation Procedure

All crowns were cemented to aged (stored in distilled water at 37°C for at least 21 days) resin composite dies (Filtek Z100, 3M ESPE). All cementation procedures followed the manufacturers' instructions. Z100 was selected as abutment material because it has an elastic modulus of 18 GPa [26, 27], which is similar to the elastic modulus of 16 – 18 GPa for human dentin [28, 29]. The effective elastic modulus of the supporting abutment and the luting cement has been found to play a governing role in the fracture resistance of the crown [30, 31].

(i) Lava Ultimate cementation: Prior to cementation all Z100 abutments were thoroughly cleaned with 70% ethyl alcohol and air dried, followed by application of Scotchbond Universal Adhesive (3M ESPE), rubbing it for 20 s and air dried for 5 s. The crowns were cleaned in ultrasonic bath and air dried. The bonding surfaces of the resin composite crowns were sandblasted using aluminum oxide particle (50 µm at 2 bars), avoiding crown margins until the entire bonding surface appears matte. Crowns were then thoroughly cleaned with 70% ethyl alcohol and air dried. Scotchbond Universal Adhesive was applied to the bonding surface of the crown, scrubbed in for 20 s, and air dried for 5 s. The luting agent used was RelyX Ultimate (3M ESPE) dispensed by the mixing tip inside the crown. The crown was then firmly seated and stabilized onto the abutment. The cement excess was chipped away after brief light curing. Polymerization of the luting agent was carried out by using a dental curing light (Ultra Lume LED 5), exposing each surface of the crown for 20 s.

(ii) IPS Empress CAD cementation: Z100 abutments were also cleaned with 70% ethyl alcohol, followed by application of Monobond Plus (Ivoclar Vivadent), 60 s waiting time, and air dried. The bonding surfaces of the crown were thoroughly cleaned with 70% ethyl alcohol, followed by application of 5% hydrofluoric acid gel (Vita Ceramics Etch - VITA) for 60 s, washed in tap water, and air dried for 20 s. Monobond Plus was applied, followed by 60 s waiting time, and air drying. The luting agent used was Multilink Automix system (Ivoclar Vivadent). The following steps were identical to those described for the resin composite crowns.

After cementation specimens were stored in distilled water at 37°C for a minimum of 5 days for polymerization and hydration of the cement layer prior to mechanical testing.

## 2.3 Mechanical Testing

**2.3.1 Single Cycle Load to Fracture Test**—To determine the accelerated sliding contact mouth-motion step-stress profiles, three crowns per group were subjected to the single cycle load to failure test [32, 33]. The crown/tooth replica assembly was mounted in a universal testing machine (Model 5566, Instron); load was applied axially through a tungsten carbide indenter ( $r = 3.18$  mm) on the central fossa of the occlusal surface using a 10 kN load cell and 1 mm/min load rate.

**2.3.2 Accelerated Sliding Contact Mouth-Motion Step-Stress Fatigue Test**—Twenty one crowns from each group were subjected to mouth-motion step-stress fatigue. Mechanical testing was performed by sliding a spherical tungsten carbide (WC) indenter ( $r$

= 3.18 mm) 0.7 mm down the distobuccal cusp towards the central fossa, using an electrodynamic fatigue testing machine (Elf-3300, Enduratec Division of Bose, Minnetonka, MN, USA). Crowns were immersed in distilled water during fatigue testing [33].

Three step-stress profiles (aggressive, moderate, and mild) were designed for fatigue testing [33]. The 21 crowns per group were distributed across the three profiles in the ratio of 1:2:4, aggressive to mild, respectively, based upon the load to fracture experiments. For the resin composite crowns the mild profile started at 400 N indentation load and went to 1200 N at 170,000 cycles; the moderate profile started at 500 N and went to 1400 N at 120,000 cycles; the aggressive profile at 600 N and went to 1700 N at 90,000 cycles. Whereas for the glass-ceramic crowns, the mild profile started with a 50 N indentation load based on the load-to-fracture experiments and load was increased by predetermined steps until fracture. Similarly, for the moderate and aggressive profiles, indentation load started at 100 N and 150 N, respectively, and was increased successively until fracture.

It is well-established that ceramic [34] and composite [35] materials are sensitive to load/stress rate. Therefore, in the current fatigue test, a clinically relevant load rate (1000 N/s) was utilized [36, 37]. As a result, the loading frequency, including load, slide and lift-off phases, varied from 0.3 Hz at 1700 N to 3 Hz at 100 N.

At the end of each load cycle, all specimens were inspected under polarized light stereomicroscopy for cracks and damage. Bulk fracture and chip-off fracture of the crowns were considered as failures. A Weibull curve and reliability for completion of a mission of 100,000 cycles were calculated (ALTA 7 PRO, Reliasoft) for the glass-ceramic group only (resin composite group did not present failures during step-stress tests).

## 2.4 Microscopic Imaging Analysis

After mouth-motion step-stress fatigue tests, all crowns that did not present fracture (from the resin composite group only) were firstly examined for occlusal surface damage associated with the fatigue scar and its surrounding areas using polarized light stereomicroscopy (Leica MZ-APO, Wetzlar, Germany). Fifteen specimens were then embedded in the clear epoxy resin, sectioned, and polished (all 12 samples from the mild profile & 3 samples from the aggressive profile) to evaluate the extent of subsurface damage. Sectioning took place along the direction of sliding contact and slightly away from the center of the fatigue scar, using a water cooled low speed diamond saw (Isomet, Buehler, Lake Buff, IL). The cross-sections were polished up to the center of the fatigue scar with a 1  $\mu$ m diamond suspension finish and analyzed using optical and scanning electron microscopes for the presence of cracks and damages. Measurements of the actual length and depth of contact-induced partial cone cracks, median cracks, inner cone cracks, and flexural-induced cementation surface radial cracks were performed using Leica QWin software in a polarized light stereomicroscope (Leica MZ-APO). In addition, scanning electron microscopy (SEM, S-3500 N, Hitachi Instruments, Tokyo, Japan) was utilized to observe the microstructure of the two materials tested and the interaction between the cracks and the microstructural features.

At the end of fatigue loading, we evaluated latent damage in survivors using a sectioning technique [38] rather than a residual strength measurement using the monotonic load to failure test [39–41]. We believe that more information was to be gleaned by identifying surface and subsurface structural changes than from very high load fracture patterns or reduction in initial strength.

### 3 Results

The microstructures of the resin composite Lava Ultimate and the glass-ceramic IPS Empress CAD are shown in Fig.1. SEM and EDS analyses revealed that the microstructure of the resin composite material consisted of a polymer matrix with high ceramic filler loading (Fig. 1a). However, due to the relatively low magnification of our SEM, only the nanoparticle clusters of silica and zirconia were observed, which were in the range of 0.6 – 10  $\mu\text{m}$ . It was not possible to identify the dispersed silica and zirconia nanoparticles described by the manufacturer of this material (silica particles  $\approx 20$  nm, zirconia particles  $\approx 4 - 11$  nm). The microstructure of the glass-ceramic consisted of a glassy matrix with evenly distributed leucite crystals (Fig. 1b). The diameter of these crystals was about 1 – 5  $\mu\text{m}$ ; the crystal content was 35 – 45 % by volume.

The results of the single cycle load to fracture test are presented in Table 1. The mean ( $\pm$  SD) critical load at fracture for resin composite crowns was  $3271 \pm 143$  N, whereas that for glass-ceramic crowns was  $1465 \pm 222$  N. Both materials, however, showed the same pattern of fracture – splitting of the crown in the middle through proximal surfaces (Fig. 2). Following mouth-motion fatigue with predetermined step-stress profiles, resin composite crowns had a survival rate of 100%, no catastrophic failures. Despite the very high indentation loads (up to 1700 N), only minor occlusal damage was observed (Fig. 3a).

Careful examination of the resin composite crowns from the occlusal aspect revealed two fatigue damage modes: sliding-contact induced occlusal surface herringbone cracks on the distobuccal cusp [31, 42]; and, impact induced concentric ring cracks on the distolingual cusp [43, 44]. Under the cyclic loading in wet environments, both herringbone and ring cracks are capable of propagating deep into the material, forming partial [26, 33] and inner cone cracks, respectively [45]. Only one crown among 21 specimens, from the aggressive profile, experienced minor spalling at the leading edge of the sliding contact (Fig. 3b).

To determine the occlusal crack depth and whether the flexure-induced cementation surface radial cracks were formed, all 12 crowns from the mild profile (higher number of loading cycles) and all 3 crowns from the aggressive profile (higher level of indentation load) were sectioned. Stereomicroscopic images showed several type of damage modes in the resin composite crowns: distobuccal cusp sliding-induced occlusal surface partial cone cracks [31] (Fig. 4a) in all sectioned crowns; median cracks [26] (Fig. 4b) in 5 crowns; distolingual cusp impact-induced inner cone cracks [46, 47] (Fig. 4c) in 7 crowns; flexure-induced cementation surface radial cracks [34, 48, 49] (Fig. 4d) in 2 crowns; and minor spalling associated with the sliding-contact fatigue scar [50] (Fig. 4e) in 1 crown.

The lengths for different types of cracks in the resin composite crowns are given in Table 2. It is important to note that the crack lengths for various crack systems were measured near the center of the fatigue scar on the cross-sectional specimens. They are not necessarily representing the longest crack length of each crack system. Fig. 5 shows one of the radial cracks observed in the resin composite crowns. This crack appeared to form at the cement/Z100 interface and was associated with a large defect in Z100 abutment which compromised the structural support of the cement layer. The crack ran across the cement layer, reinitiated in the resin composite crown structure, and propagated upward and sideward. Quantitative imaging analysis showed the crack length to be about 1000  $\mu\text{m}$ , about half the thickness of the crown.

SEM micrographs showing the interaction between the crack and the microstructure of the resin composite material appear in Fig. 6. Lava Ultimate restorative is a blend of 80 wt.% ceramic fillers embedded in a highly cured resin matrix. The ceramic fillers are made up of three different ceramic particles: highly dispersed silica particles (20 nm) and zirconia particles (4 – 11 nm), and aggregated zirconia/silica clusters (0.6 – 10  $\mu\text{m}$ ), comprised of 20 nm silica and 4 to 11 nm zirconia particles. At the micro-fracture scale, crack interaction with the zirconia/silica clusters varied with the crack incidence angle. When the crack intersected the nanoparticle cluster at an acute angle, it often propagated or deflected around the cluster (Fig.6a), suggesting some toughening mechanisms in these highly filled resin composites. However, when the crack encountered the cluster at a high angle, the crack penetrated through the nanoparticle cluster (Fig. 6b).

Using a cumulative damage model with power law relationship, the 2-parameter Weibull load – failure probability plot was generated for the glass-ceramic crowns using the mouth-motion step-stress fatigue data (Fig. 7). Reliability (two-sided at 90% confidence bounds) for completion of a mission of 100,000 cycles at 400 N indentation load was 0.773 (0.867 – 0.6273). However, when the indentation load was increased to 600 N, reliability was reduced to 0.171 (0.293 – 0.079). At a clinically relevant load of 200 N, the survivability of IPS Empress CAD molar crowns was 90% at 1,250,000 cycles, which simulates ~5 years in vivo.

Stereomicroscope images of a typical fracture pattern in the glass-ceramic crowns are shown in Fig. 8 (a) occlusal view and (b) buccal view. In this specimen, fracture occurred following mouth-motion step-stress fatigue at 475 N/220,000 cycles. The fracture had a typical scallop-shaped morphology with a maximum length (measuring from the occlusal surface down the buccal wall toward margin) of approximately 5 mm and a width in the disto-mesial direction of approximately 5.5 mm. Closer inspection from the buccal aspect of the crown (Fig. 8b) revealed multiple arrest lines, suggesting the fracture originated at the occlusal contact point. The fractured surface did not expose the Z100 abutment. In most of the fractured glass-ceramic crowns, the chip-off fracture involved two cusps (distobuccal cusp and distal cusp). To confirm that glass-ceramic crowns failed exclusively from the chip-off fracture associated with the occlusal contact, 8 crowns (especially those fractured at higher indentation loads, i.e. > 550 N) were sectioned along the sliding contact direction and across the fatigue scar. No radial fractures were observed.

During the mouth-motion step-stress fatigue of the glass-ceramic crowns, cracks initiated at the occlusal contact area and propagated as the indentation load and number of loading cycles increased. Once these cracks reached a critical size (often longer than 5 mm), the next loading step then often resulted in chip-off fracture. Two crowns that developed extensive crack formation were sectioned before a chip-off fracture occurred. Both of these cracks extended deep into the material, reaching the crown-cement-abutment interface (Fig. 8d).

## 4 Discussion

This *in vitro* study investigated the sliding-contact fatigue resistance and damage modes of a recently developed indirect resin composite for CAD/CAM applications. The results support the hypothesis that CAD/CAM resin composite molar crowns have better fatigue fracture resistance than leucite reinforced glass-ceramic molar crowns. Following the most harsh stepstress profiles that the chewing simulator could deliver (a maximum fatigue load of 1700 N), none of the resin composite crowns experienced catastrophic failure. By contrast, no sample from the leucite glass-ceramic group survived at 650 N indentation loads.

Damage modes sustained in the CAD/CAM resin composite crown/abutment system have been investigated: sliding-contact induced partial cone cracks and impact induced inner cone cracks initiated at the occlusal surface and propagated into but not through the restorative material (observed in all cases). Flexure-induced radial cracks, only observed in two cases, initiated at the cementation surface. While three crack modes have been identified, the cracks were relatively small compared to the crown thickness even after 1200 N and 170,000 loading cycles. Sliding contact partial cone cracks (100 – 500  $\mu\text{m}$ ), which are about 1/10 – 1/4 of crown thickness (2000  $\mu\text{m}$ ). Impact induced inner cone cracks (100 – 300  $\mu\text{m}$ ) that are about 1/10 – 1/5 of the same crown thickness. Two cases of radial cracks, however, are approximately 1/10 and 1/2 of the crown thickness, respectively. The propagation of these near-contact induced cone cracks and far-field flexural radial cracks leading to chip-off and bulk fractures of the indirect resin composite crowns would require higher indentation loads or larger number of loading cycles [51].

The glass ceramic crowns all failed in the form of chip-off fractures during mouth-motion step-stress fatigue at an indentation load level of 450 N or higher. A 90% survival rate was estimated for a mission of 1,250,000 cycles at 200 N, which is equivalent to ~5 years of clinical survival in occlusal function [52, 53]. A systematic review by Heintze and Rousson [54] included seven clinical studies involving 1,487 adhesively luted IPS Empress crowns concluded that the hazard for failure for these crowns was 16 in every 1,000 crowns per year for molars. This indicates that Empress CAD crowns have good clinical performance, with the main reported cause for clinical failure being chipping fractures. Similarly, in the present study, all glass-ceramic crowns failed by chipping fractures, indicating some clinical relevance of the applied test set-up.

These results are consistent with other studies showing mechanical robustness of indirect resin composite materials compared to ceramic materials. Magne and coworkers [20, 21] conducted series of studies on the fatigue fracture resistance of CAD/CAM resin composite (Paradigm MZ100). They showed that the fatigue resistance of Paradigm MZ100 posterior



occlusal veneers with various thicknesses outperformed their ceramic (IPS Empress CAD or IPS e.max CAD) counterparts. Present findings are also supported by Johnson et al. [25], who determined the effect of material type and restoration thickness on the fracture strength of posterior occlusal veneers made from computer-milled resin composite materials (Paradigm MZ100 and Lava Ultimate). The authors reported that occlusal veneers made from the resin composites tested are likely to survive the occlusal forces regardless of restoration thickness, with those fabricated from Lava Ultimate being more likely to survive higher loads [25]. Kassem et al. [23] also studied the effect of compressive cyclic loading on the fatigue resistance and microleakage of monolithic CAD/CAM molar ceramic and resin composite crowns, and observed that all resin composite crowns survived after 1,000,000 cycles of compressive cyclic loading, more fatigue resistance than VMII (VITABLOCK Mark II) ceramic crowns.

The main reasons possibly related to the excellent fatigue reliability of the CAD/CAM nanohybrid resin composite in this study are: Firstly, high filler loading which is made possible by a hybrid structure consisting of extremely small discrete nanoscale particles (4 – 20 nm) and clusters of nanoparticles (0.6 – 10  $\mu\text{m}$ ) [55]; Secondly, the CAD/CAM process uses blocks, which are manufactured under the standard conditions, producing a more homogeneous, dense and reliable material [12]; Finally, due to the similar elastic modulus of the restorative material to the effective modulus of abutment (Z100) and of the resin-based cement, extremely high indentation loads are required to initiate flexural-induced radial cracks at the cementation surface.

The results of this *in vitro* study have demonstrated that indirect resin composite molar crowns have excellent resistance to contact fatigue damage. These findings suggest a level of fracture resistance that may be clinically acceptable. Since molar crowns are subjected to high chewing stresses, they are vulnerable to fracture. Therefore, this newly developed CAD/CAM nanohybrid material can be indicated for posterior crown applications as it meets the mechanical requirements for high stress bearing areas. Until now, no clinical studies for this crown material have been published to confirm this assumption.

During the development of this manuscript, 3M ESPE has announced the removal of the full coverage crown indication for Lava Ultimate due to a higher than anticipated debonding issue, whereas this product continues to be indicated for inlays, onlays, and veneer restorations. Since Lava Ultimate has demonstrated a superior resistance to fatigue fracture, future research should focus on the resin bond property of this material in order to extend its clinical indications to full coverage crowns.

Due to the high fatigue fracture resistance presented by Lava Ultimate crowns, this material may be indicated for patients with parafunctional activity. Manifestation of bruxism can be as grinding or clenching, both generating high loads/stresses onto the dental structures and restorations. Although Lava Ultimate CAD/CAM Restorative was able to withstand parafunctional-like high occlusal loading, it would still be a challenge to test these materials in overlay restorations when patients with severe tooth wear need to be restored in increased vertical dimension by a minimally invasive tooth preparation. In those bruxing patients, grinding comprises the majority of the sliding component of chewing (i.e. no food bolus

between teeth, thus causing direct tooth to tooth contact). Tooth loading at 1000 – 1400 N would correspond to extreme situations with high extrinsic forces (trauma) [22, 56] or intrinsic masticatory accidents (under chewing loads but delivered to a small area due to a hard foreign body such as a pit or seed, for example). However, when the restorative design is changed from a crown towards a less retentive overlay restoration, more attention has to be paid to the quality of the cement-interface and minimal thickness of the material as this might influence the strength of the tooth restorative complex [57].

While it is clear that composites can undergo degradations in structural and bonding properties due to temperature, pH, and bacterial and enzymatic activities [58–60], such multifactorial effects were beyond the scope of this study. We feel that it is extremely important to first establish the true fatigue performance of the composites before any significant degradation occurs. The results obtained from such study can serve as a reference for comparison with future multifactorial studies.

The accelerated step-stress fatigue test has been used to predict the failure probability of dental restorative materials by various research groups [61–63]. This method has been validated by *in vitro* tests [62] and step-stress fatigue failure modes mimicked those seen clinically [64, 65]. Based on these observations, the objective of this study was to elucidate the fatigue behavior of CAD/CAM resin-based composite relative to glass-ceramic molar crowns. Ultimately, clinical trials will be needed to establish whether these materials are able to function clinically.

## 5 Conclusions

Monolithic Lava Ultimate resin composite CAD/CAM crowns can endure exceptionally high fatigue loads. Several fatigue damage modes were noted: sliding-induced partial cone cracks, impact-induced inner cone cracks, and flexure-induced cementation surface radial cracks. All of these damages were contained within the restoration. None of these resin composite crowns exhibited catastrophic failure. Under present conditions, this nanohybrid indirect resin composite material meets the mechanical requirements for high stress-bearing posterior restorations, showing excellent resistance to contact and flexural damage. If bonding issues can be resolved, they offer an aesthetic option for damage-resistant crowns in the posterior regions of the mouth.

## Supplementary Material

Refer to Web version on PubMed Central for supplementary material.

## Acknowledgments

Certain results of this study (i.e. fatigue of Lava Ultimate crowns) were submitted as part of a Master's thesis by F. Shembish in partial fulfillment of the requirements for a Master of Science degree. This work was sponsored by funding from the United States National Institute of Dental & Craniofacial Research, National Institutes of Health (P.I. Y. Zhang, Grant 2R01 DE017925).

## References

1. Heintze SD, Rousson V. Clinical effectiveness of direct class ii restorations - a meta-analysis. *J Adhes Dent.* 2012; 14:407–431. [PubMed: 23082310]
2. Lynch CD, Opdam NJ, Hickel R, Brunton PA, Gurgan S, Kakaboura A, Shearer AC, Vanherle G, Wilson NH. Guidance on posterior resin composites: Academy of operative dentistry - european section. *J Dent.* 2014; 42:377–383. [PubMed: 24462699]
3. Opdam NJ, van de Sande FH, Bronkhorst E, Cenci MS, Bottenberg P, Pallesen U, Gaengler P, Lindberg A, Huysmans MC, van Dijken JW. Longevity of posterior composite restorations: A systematic review and meta-analysis. *J Dent Res.* 2014; 93:943–949. [PubMed: 25048250]
4. Pjetursson BE, Sailer I, Zwahlen M, Hammerle CH. A systematic review of the survival and complication rates of all-ceramic and metal-ceramic reconstructions after an observation period of at least 3 years. Part i: Single crowns. *Clin Oral Implants Res.* 2007; 18(Suppl 3):73–85. [PubMed: 17594372]
5. Wittneben JG, Wright RF, Weber HP, Gallucci GO. A systematic review of the clinical performance of CAD/CAM single-tooth restorations. *Int J Prosthodont.* 2009; 22:466–471. [PubMed: 20095195]
6. Jongsma LA, Kleverlaan CJ, Feilzer AJ. Clinical success and survival of indirect resin composite crowns: Results of a 3-year prospective study. *Dent Mater.* 2012; 28:952–960. [PubMed: 22608959]
7. van Dijken JW. Direct resin composite inlays/onlays: An 11 year follow-up. *J Dent.* 2000; 28:299–306. [PubMed: 10785294]
8. Fennis WM, Kuijs RH, Roeters FJ, Creugers NH, Kreulen CM. Randomized control trial of composite cuspal restorations: Five-year results. *J Dent Res.* 2014; 93:36–41. [PubMed: 24155264]
9. Christensen GJ. Porcelain-fused-to-metal vs. Nonmetal crowns. *J Am Dent Assoc.* 1999; 130:409–411. [PubMed: 10085664]
10. Trajtenberg CP, Caram SJ, Kiat-amnuay S. Microleakage of all-ceramic crowns using self-etching resin luting agents. *Oper Dent.* 2008; 33:392–399. [PubMed: 18666496]
11. Kunzelmann KH, Jelen B, Mehl A, Hickel R. Wear evaluation of mz100 compared to ceramic CAD/CAM materials. *Int J Comput Dent.* 2001; 4:171–184. [PubMed: 11862884]
12. Giordano R. Materials for chairside CAD/CAM-produced restorations. *JADA.* 2006; 137(9 supplement):14S–21S. [PubMed: 16950933]
13. Gary Davidowitz PGK. The use of CAD/CAM in dentistry. *Dent clin N Am.* 2011; 55:559–570. [PubMed: 21726690]
14. Mormann WHBM, Lutz F, Barbakow F. Chairside computer-aided direct ceramic inlays. *Quintessence Int.* 1989; 20:329–339. [PubMed: 2756089]
15. Kaizer MR, de Oliveira-Ogliari A, Cenci MS, Opdam NJM, Moraes RR. Do nanofill or submicron composites show improved smoothness and gloss? A systematic review of in vitro studies. *Dent Mater.* 2014; 30:E41–E78. [PubMed: 24529799]
16. Ferracane JL. Resin composite--state of the art. *Dent Mater.* 2011; 27:29–38. [PubMed: 21093034]
17. Ferracane JL. Resin-based composite performance: Are there some things we can't predict? *Dent Mater.* 2013; 29:51–58. [PubMed: 22809582]
18. Rueggeberg FA. State-of-the-art: Dental photocuring--a review. *Dent Mater.* 2011; 27:39–52. [PubMed: 21122903]
19. Stansbury JW. Dimethacrylate network formation and polymer property evolution as determined by the selection of monomers and curing conditions. *Dent Mater.* 2012; 28:13–22. [PubMed: 22192248]
20. Magne P, Schlichting LH, Maia HP, Baratieri LN. In vitro fatigue resistance of CAD/CAM composite resin and ceramic posterior occlusal veneers. *J Prosthet Dent.* 2010; 104:149–157. [PubMed: 20813228]
21. Schlichting LH, Maia HP, Baratieri LN, Magne P. Novel-design ultra-thin CAD/CAM composite resin and ceramic occlusal veneers for the treatment of severe dental erosion. *J Prosthet Dent.* 2011; 105:217–226. [PubMed: 21458646]

22. Magne P, Knezevic A. Simulated fatigue resistance of composite resin versus porcelain CAD/CAM overlay restorations on endodontically treated molars. *Quintessence Int.* 2009; 40:125–133. [PubMed: 19169444]
23. Kassem AS, Atta O, El-Mowafy O. Fatigue resistance and microleakage of CAD/CAM ceramic and composite molar crowns. *J Prosthodont.* 2012; 21:28–32. [PubMed: 22008462]
24. Belli R, Geinzer E, Muschweck A, Petschelt A, Lohbauer U. Mechanical fatigue degradation of ceramics versus resin composites for dental restorations. *Dent Mater.* 2014; 30:424–432. [PubMed: 24553249]
25. Johnson AC, Versluis A, Tantbirojn D, Ahuja S. Fracture strength of CAD/CAM composite and composite-ceramic occlusal veneers. *J Prosthodont Res.* 2014; 58:107–114. [PubMed: 24636368]
26. Kim JW, Kim JH, Thompson VP, Zhang Y. Sliding contact fatigue damage in layered ceramic structures. *J Dent Res.* 2007; 86:1046–1050. [PubMed: 17959894]
27. Zhang Y, Kim JW, Bhowmick S, Thompson VP, Rekow ED. Competition of fracture mechanisms in monolithic dental ceramics: Flat model systems. *J Biomed Mater Res B Appl Biomater.* 2009; 88:402–411. [PubMed: 18478533]
28. Kinney JH, Marshall SJ, Marshall GW. The mechanical properties of human dentin: A critical review and re-evaluation of the dental literature. *Crit Rev Oral Biol Med.* 2003; 14:13–29. [PubMed: 12764017]
29. Lawn BR, Deng Y, Lloyd IK, Janal MN, Rekow ED, Thompson VP. Materials design of ceramic-based layer structures for crowns. *J Dent Res.* 2002; 81:433–438. [PubMed: 12097438]
30. Ma L, Guess PC, Zhang Y. Load-bearing properties of minimal-invasive monolithic lithium disilicate and zirconia occlusal onlays: Finite element and theoretical analyses. *Dent Mater.* 2013; 29:742–751. [PubMed: 23683531]
31. Zhang Y, Kim JW, Kim JH, Lawn BR. Fatigue damage in ceramic coatings from cyclic contact loading with a tangential component. *J Am Ceram Soc.* 2008; 91:198–202.
32. Coelho PG, Bonfante EA, Silva NR, Rekow ED, Thompson VP. Laboratory simulation of Y-TZP all-ceramic crown clinical failures. *J Dent Res.* 2009; 88:382–386. [PubMed: 19407162]
33. Guess PC, Zavanelli RA, Silva NR, Bonfante EA, Coelho PG, Thompson VP. Monolithic CAD/CAM lithium disilicate versus veneered Y-TZP crowns: Comparison of failure modes and reliability after fatigue. *Int J Prosthodont.* 2010; 23:434–442. [PubMed: 20859559]
34. Zhang Y, Lawn B. Long-term strength of ceramics for biomedical applications. *J Biomed Mater Res B Appl Biomater.* 2004; 69:166–172. [PubMed: 15116406]
35. Du J, Niu X, Soboyejo W. Creep-assisted slow crack growth in bio-inspired dental multilayers. *J Mech Behav Biomed Mater.* 2015; 46:41–48. [PubMed: 25771255]
36. Kim JH, Kim JW, Myoung SW, Pines M, Zhang Y. Damage maps for layered ceramics under simulated mastication. *J Dent Res.* 2008; 87:671–675. [PubMed: 18573989]
37. Kim JW, Kim JH, Janal MN, Zhang Y. Damage maps of veneered zirconia under simulated mastication. *J Dent Res.* 2008; 87:1127–1132. [PubMed: 19029080]
38. Kim B, Zhang Y, Pines M, Thompson VP. Fracture of porcelain-veneered structures in fatigue. *J Dent Res.* 2007; 86:142–146. [PubMed: 17251513]
39. Heintze SD, Cavalleri A, Zellweger G, Buchler A, Zappini G. Fracture frequency of all-ceramic crowns during dynamic loading in a chewing simulator using different loading and luting protocols. *Dent Mater.* 2008; 24:1352–1361. [PubMed: 18433859]
40. Skouridou N, Pollington S, Rosentritt M, Tsitrou E. Fracture strength of minimally prepared all-ceramic cerec crowns after simulating 5 years of service. *Dent Mater.* 2013; 29:e70–e77. [PubMed: 23618556]
41. Zhao K, Wei YR, Pan Y, Zhang XP, Swain MV, Guess PC. Influence of veneer and cyclic loading on failure behavior of lithium disilicate glass-ceramic molar crowns. *Dent Mater.* 2014; 30:164–171. [PubMed: 24331550]
42. Ren L, Zhang Y. Sliding contact fracture of dental ceramics: Principles and validation. *Acta Biomater.* 2014; 10:3243–3253. [PubMed: 24632538]
43. Zhang Y, Bhowmick S, Lawn BR. Competing fracture modes in brittle materials subject to concentrated cyclic loading in liquid environments: Monoliths. *J Mater Res.* 2005; 20:2021–2029.

44. Zhang Y, Song JK, Lawn BR. Deep-penetrating conical cracks in brittle layers from hydraulic cyclic contact. *J Biomed Mater Res B Appl Biomater.* 2005; 73:186–193. [PubMed: 15672403]
45. Zhang Y, Sailer I, Lawn BR. Fatigue of dental ceramics. *J Dent.* 2013; 41:1135–1147. [PubMed: 24135295]
46. Bhowmick S, Zhang Y, Lawn BR. Competing fracture modes in brittle materials subject to concentrated cyclic loading in liquid environments: Bilayer structures. *J Mater Res.* 2005; 20:2792–2800.
47. Hermann I, Bhowmick S, Zhang Y, Lawn BR. Competing fracture modes in brittle materials subject to concentrated cyclic loading in liquid environments: Trilayer structures. *J Mater Res.* 2006; 21:512–521.
48. Rekow D, Zhang Y, Thompson V. Can material properties predict survival of all-ceramic posterior crowns? *Compend Contin Educ Dent.* 2007; 28:362–368. quiz 369, 386. [PubMed: 17687898]
49. Zhang Y, Lawn B. Competing damage modes in all-ceramic crowns: Fatigue and lifetime. *Bioceramics.* 2005; 17:697–700. 17.
50. Zhang Y, Kim JW. Graded zirconia glass for resistance to veneer fracture. *J Dent Res.* 2010; 89:1057–1062. [PubMed: 20651092]
51. Kim JW, Thompson VP, Rekow ED, Jung YG, Zhang Y. Fracture modes in curved brittle layers subject to concentrated cyclic loading in liquid environments. *J Mater Res.* 2009; 24:1075–1081. [PubMed: 26028811]
52. DeLong R, Douglas WH. Development of an artificial oral environment for the testing of dental restoratives: Bi-axial force and movement control. *J Dent Res.* 1983; 62:32–36. [PubMed: 6571851]
53. Krejci I, Lutz F. in-vitro test results of the evaluation of dental restoration systems. Correlation with in-vivo results. *Schweiz Monatsschr Zahnmed.* 1990; 100:1445–1449. [PubMed: 2277977]
54. Heintze SD, Rousson V. Fracture rates of ips empress all-ceramic crowns--a systematic review. *Int J Prosthodont.* 2010; 23:129–133. [PubMed: 20305850]
55. Beun S, Glorieux T, Devaux J, Vreven J, Leloup G. Characterization of nanofilled compared to universal and microfilled composites. *Dent Mater.* 2007; 23:51–59. [PubMed: 16423384]
56. Magne P, Knezevic A. Influence of overlay restorative materials and load cusps on the fatigue resistance of endodontically treated molars. *Quintessence Int.* 2009; 40:729–737. [PubMed: 19862399]
57. Hamburger JT, Opdam NJ, Bronkhorst EM, Huysmans MC. Indirect restorations for severe tooth wear: Fracture risk and layer thickness. *J Dent.* 2014; 42:413–418. [PubMed: 24120523]
58. Drummond JL. Degradation, fatigue, and failure of resin dental composite materials. *J Dent Res.* 2008; 87:710–719. [PubMed: 18650540]
59. Gonzalez-Bonet A, Kaufman G, Yang Y, Wong C, Jackson A, Huyang G, Bowen R, Sun J. Preparation of dental resins resistant to enzymatic and hydrolytic degradation in oral environments. *Biomacromolecules.* 2015; 16:3381–3388. [PubMed: 26358180]
60. Lohbauer U, Belli R, Ferracane JL. Factors involved in mechanical fatigue degradation of dental resin composites. *J Dent Res.* 2013; 92:584–591. [PubMed: 23694927]
61. Baldassarri M, Zhang Y, Thompson VP, Rekow ED, Stappert CF. Reliability and failure modes of implant-supported zirconium-oxide fixed dental prostheses related to veneering techniques. *J Dent.* 2011; 39:489–498. [PubMed: 21557985]
62. Borba M, Cesar PF, Griggs JA, Della Bona A. Step-stress analysis for predicting dental ceramic reliability. *Dent Mater.* 2013; 29:913–918. [PubMed: 23827018]
63. Coelho PG, Silva NR, Bonfante EA, Guess PC, Rekow ED, Thompson VP. Fatigue testing of two porcelain-zirconia all-ceramic crown systems. *Dent Mater.* 2009; 25:1122–1127. [PubMed: 19395078]
64. Pang Z, Chughtai A, Sailer I, Zhang Y. A fractographic study of clinically retrieved zirconia-ceramic and metal-ceramic fixed dental prostheses. *Dent Mater.* 2015; 31:1198–1206. [PubMed: 26233469]
65. Silva NR, Bonfante EA, Zavanelli RA, Thompson VP, Ferencz JL, Coelho PG. Reliability of metaloceramic and zirconia-based ceramic crowns. *J Dent Res.* 2010; 89:1051–1056. [PubMed: 20660796]

### Highlights

- Monolithic Lava Ultimate resin composite CAD/CAM crowns can tolerate fatigue loads 3 – 4 times higher than those causing catastrophic failure in IPS Empress CAD glass-ceramic crowns.
- Lava Ultimate resin composite crowns seem to offer an aesthetic option for damage-resistant restorations in the posterior regions.
- This nanohybrid indirect resin composite material meets the mechanical requirements for high stress-bearing posterior restorations; future development should focus on the improvement in its cement bond properties.

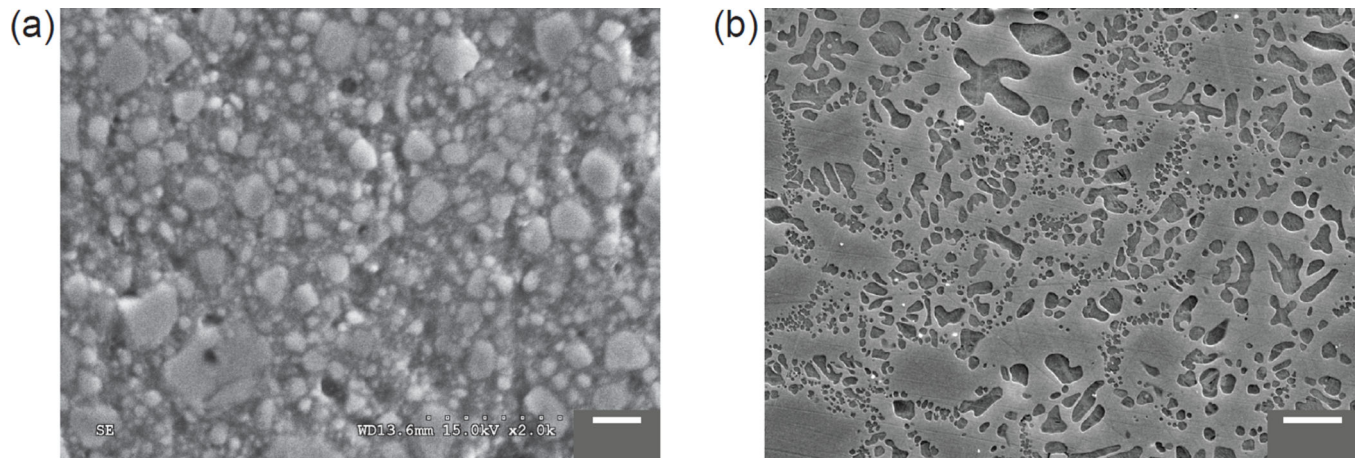


**Figure 1.** Microstructure of the resin composite Lava Ultimate (left) and the glass-ceramic IPS Empress CAD (right, courtesy of Ivoclar). Both materials were polished down to 1  $\mu\text{m}$  prior to imaging. In addition, IPS Empress CAD surface was acid etched with 40% hydrofluoric vapor (20 s) to allow a better examination of the crystalline content.

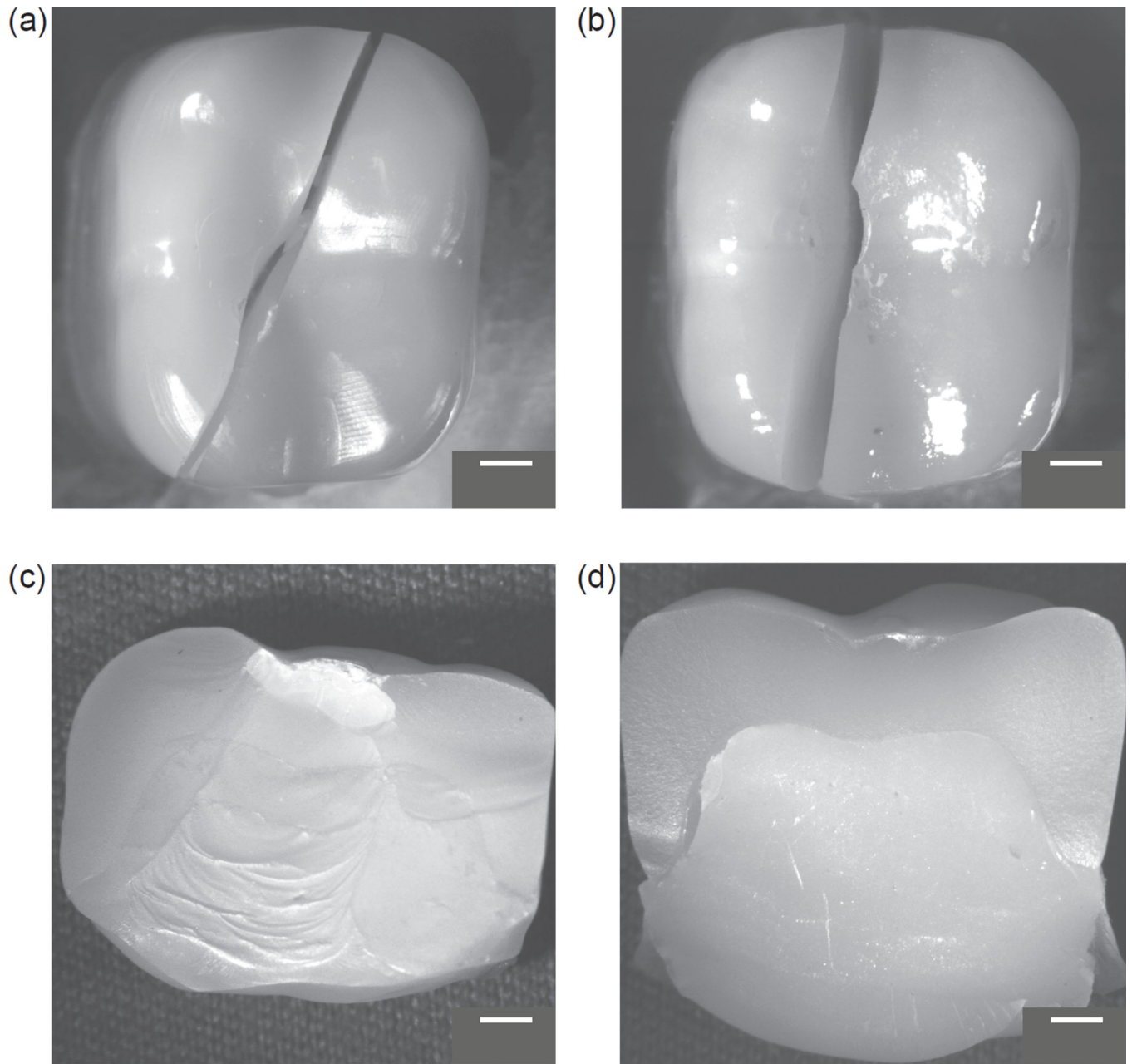


**Figure 2.** Single cycle load-to-failure fracture modes. (a,c) Resin composite crown ( $3271 \pm 143$  N); (b,d) Glass-ceramic crown ( $1465 \pm 222$  N).



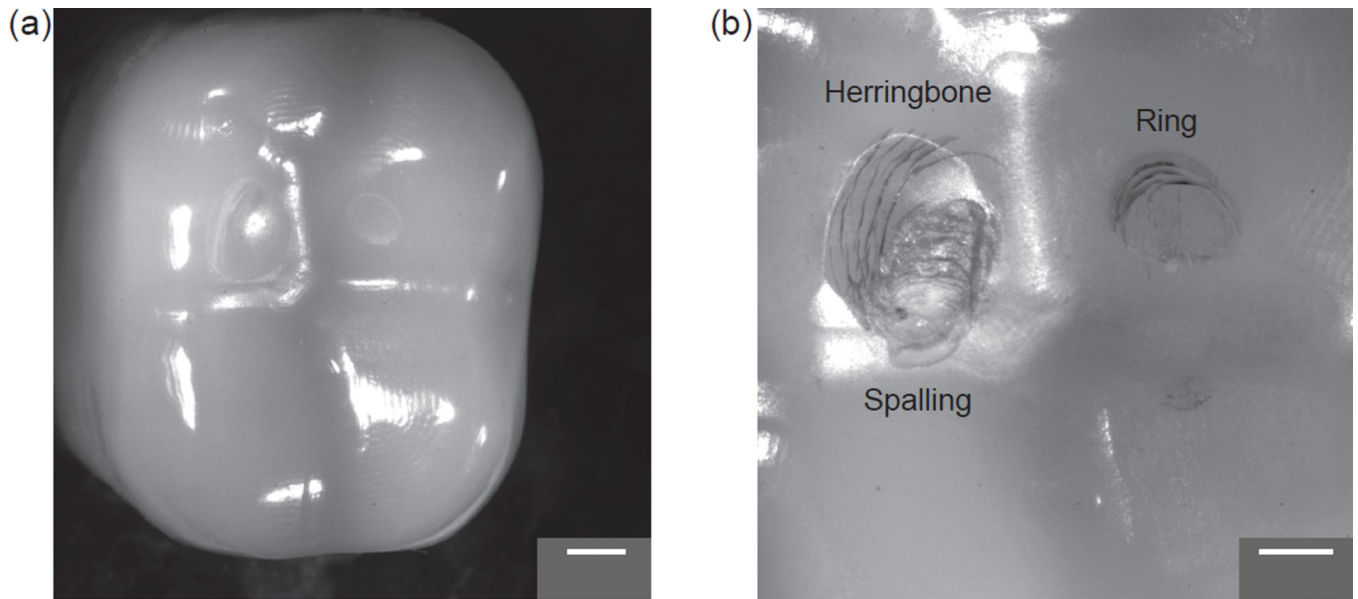


**Figure 3.** (a) Occlusal view of a resin composite crown from the mild profile (indentation load of 1200 N at 170K loading cycles). (b) Details of the fatigue scar in a resin composite crown from the aggressive profile (indentation load of 1700 N at 90K cycles). Note in (b): minor spalling measuring 1255  $\mu\text{m}$  and 1796  $\mu\text{m}$  in the bucco-lingual and mesio-distal directions, respectively.

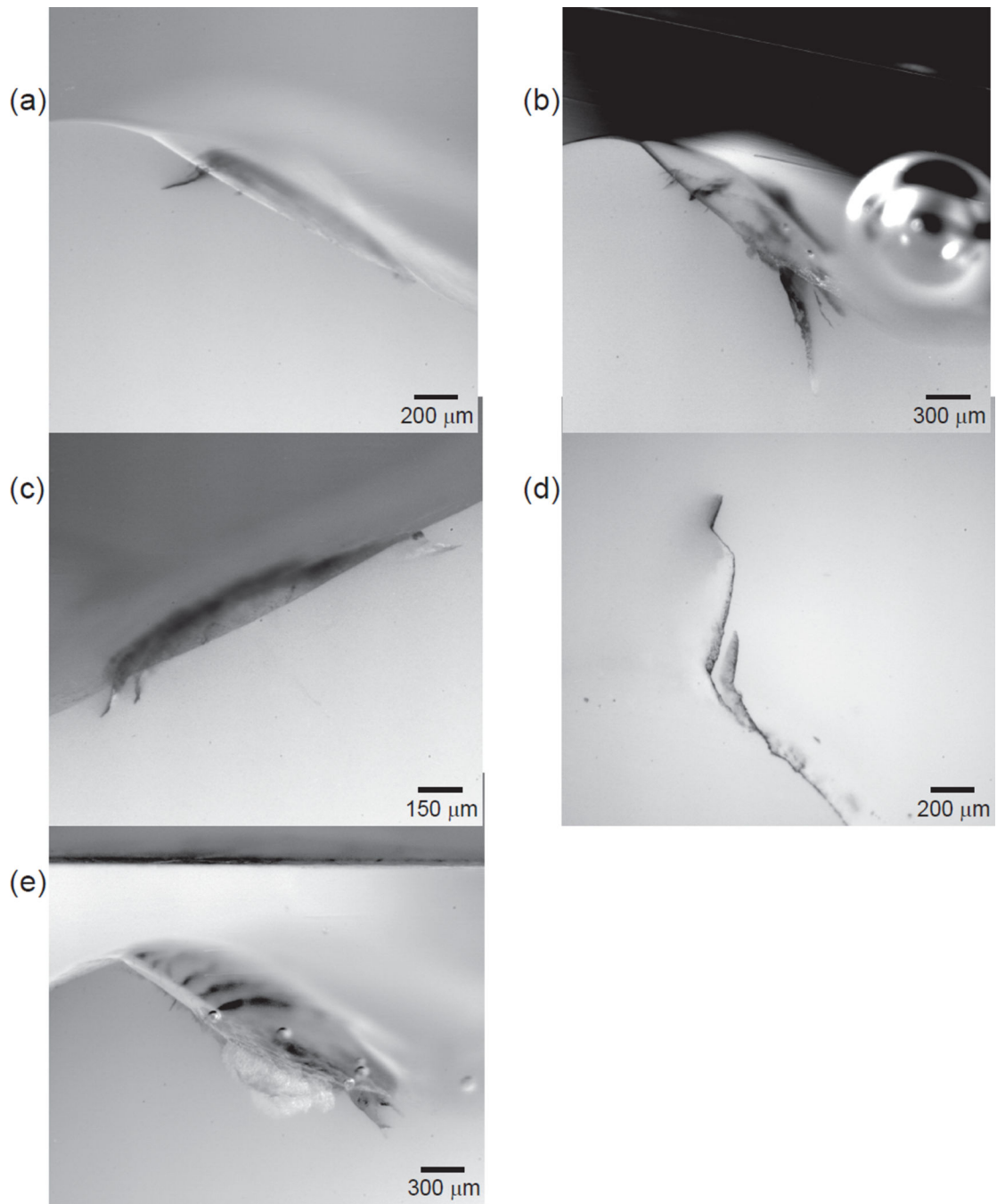


**Figure 4.** Damage modes in resin composite crowns. (a) Sliding contact induced partial cone cracks. (b) Occlusal contact induced median cracks. (c) Impact induced inner cone cracks. (d) Flexure induced cementation surface radial cracks. (e) Minor spalling (Depth ~300 μm).

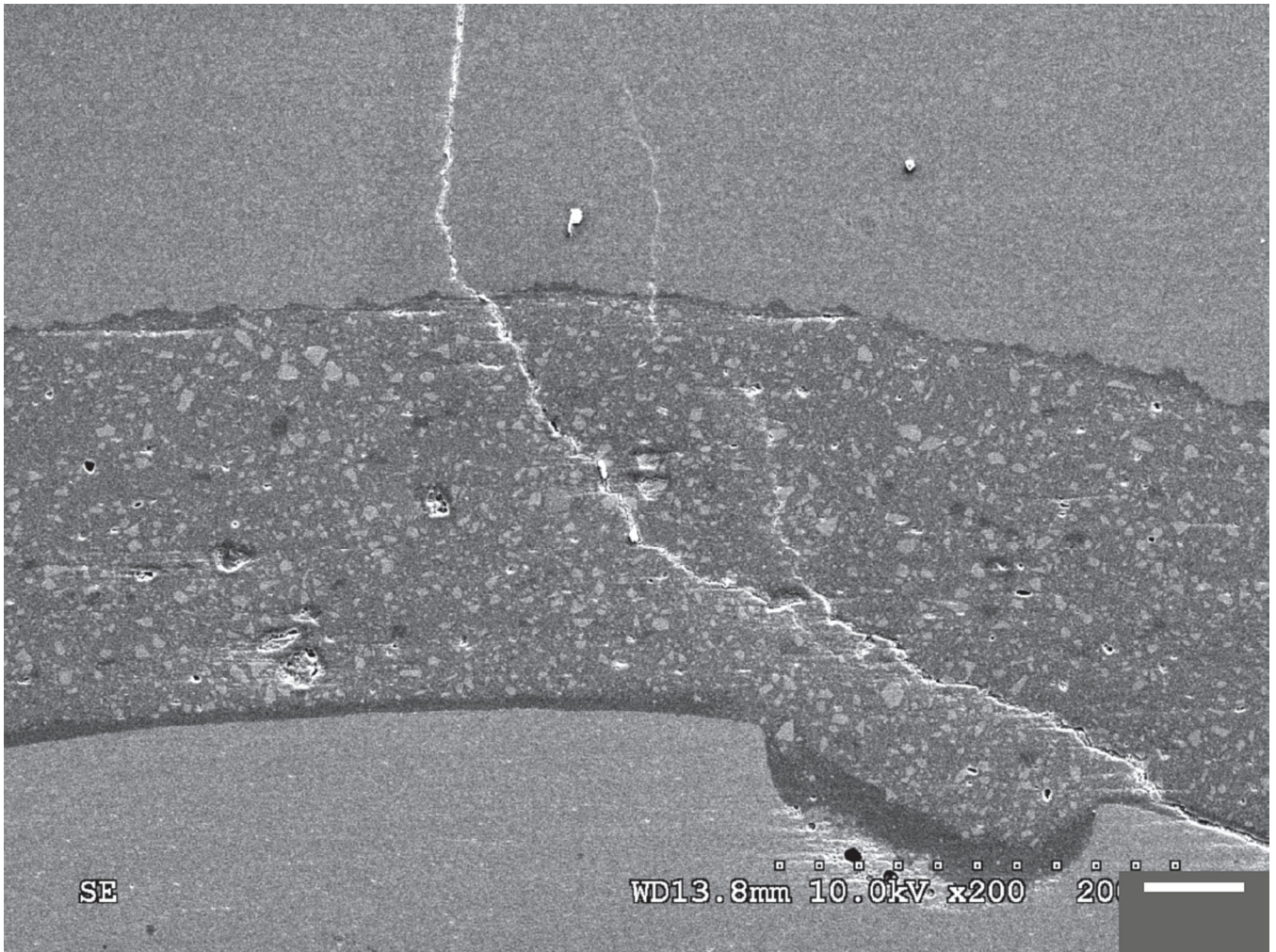


**Figure 5.** Flexure induced radial crack in a resin composite crown. Note: a large defect in the abutment compromises the support for the cement.

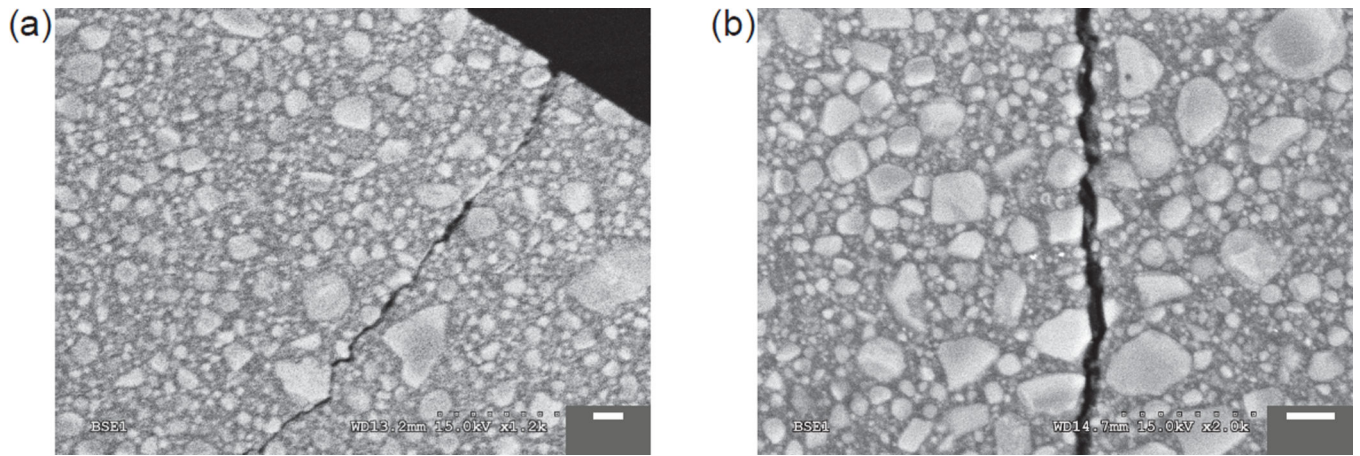


**Figure 6.**  
Crack interactions with nanoparticle clusters in the resin composite.

Author Manuscript

Author Manuscript

Author Manuscript

Author Manuscript

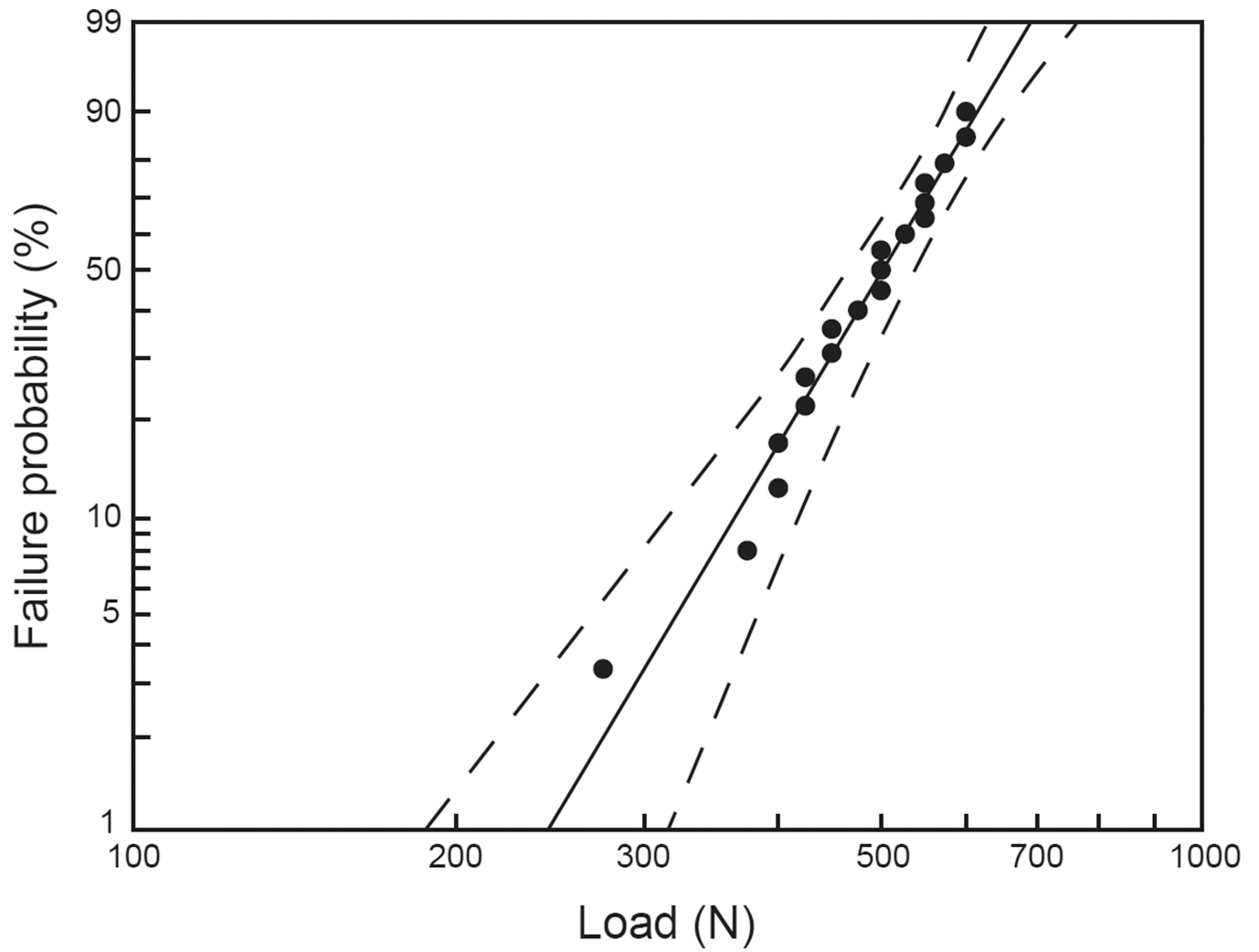


**Figure 7.** IPS Empress CAD failure probability (Weibull distribution) versus load with 90% two-sided confidence bounds (dashed lines).

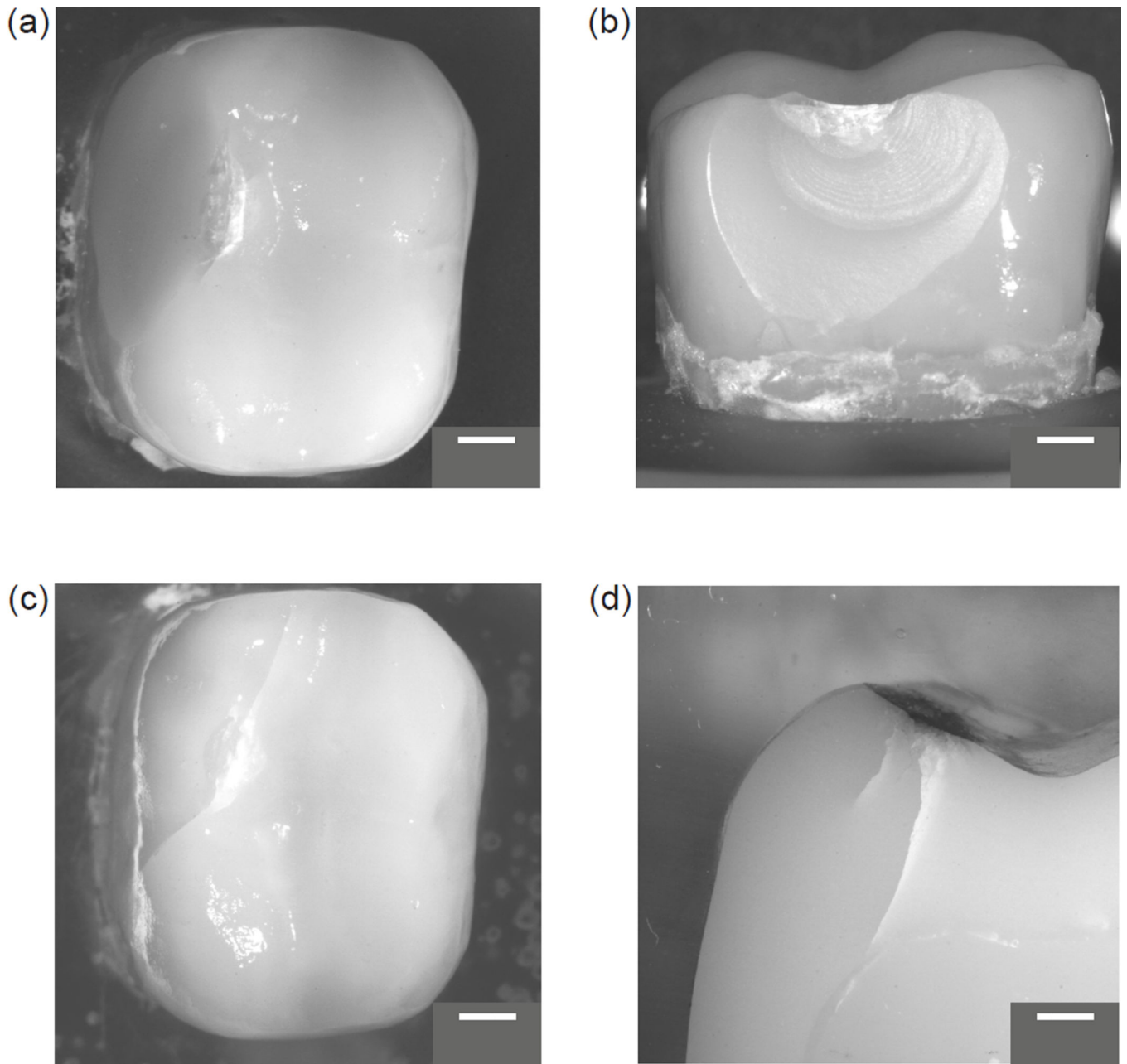


**Figure 8.**

(a) Occlusal view and (b) buccal view of a typical fracture pattern of the glass-ceramic materials (indentation load of 475 N at 220,000 loading cycles). (c) Occlusal view and (d) section view of a glass-ceramic crown (indentation load of 550 N at 250,000 loading cycles) exhibiting extensive crack formation.

**Table 1**

Maximum flexure load (N) for three specimens of each group.

	<b>Lava Ultimate</b>	<b>IPS Empress CAD</b>
Load (N)	3378	1275
	3325	1410
	3108	1709
Mean $\pm$ SD (N)	3271 $\pm$ 143	1465 $\pm$ 222

Author Manuscript

Author Manuscript

Author Manuscript

Author Manuscript

**Table 2**

Lava Ultimate CAD crack modes and length

Lava Ultimate Sample (Mild Profile)	Sliding Induced Occlusal Cracks		Impact Induced Inner Cone Cracks	Flexural Cementation Surface Radial Cracks beneath Impact Cusp
	Occlusal Surface Partial Cone Cracks	Median Cracks		
Sample 1	219 $\mu\text{m}$	146 $\mu\text{m}$	142 $\mu\text{m}$	×
Sample 2	117 $\mu\text{m}$	965 $\mu\text{m}$	×	1/10 of crown thickness (180 $\mu\text{m}$ )
Sample 3	421 $\mu\text{m}$	×	×	×
Sample 4	365 $\mu\text{m}$	×	207 $\mu\text{m}$	1/2 of crown thickness (1006 $\mu\text{m}$ )
Sample 5	269 $\mu\text{m}$	×	127 $\mu\text{m}$	×
Sample 6	158 $\mu\text{m}$	×	×	×
Sample 7	168 $\mu\text{m}$	467 $\mu\text{m}$	×	×
Sample 8	268 $\mu\text{m}$	195 $\mu\text{m}$	129 $\mu\text{m}$	×
Sample 9	162 $\mu\text{m}$	×	108 $\mu\text{m}$	×
Sample 10	251 $\mu\text{m}$	×	296 $\mu\text{m}$	×
Sample 11	326 $\mu\text{m}$	×	×	×
Sample 12	230 $\mu\text{m}$	×	×	×